JOURNAL OF SOLID STATE CHEMISTRY 110, 100–105 (1994)

The Defect Chemistry of $LaMnO_{3\pm\delta}$*

2. Structural Aspects of $LaMnO_{3+\delta}$

J. A. M. Van Roosmalen, E. H. P. Cordfunke, and R. B. Helmholdt

Netherlands Energy Research Foundation ECN, P.O. Box 1, 1755 ZG Petten, The Netherlands

and

H. W. Zandbergen

National Centre for High Resolution Electron Microscopy, Delft University of Technology, Rotterdamseweg 137, 2628 AL Delft, The Netherlands

Received August 14, 1992; in revised form February 3, 1993; accepted February 8, 1993

The overall defects in $LaMnO_{3+\delta}$ have been studied by powder neutron diffraction, electron diffraction, and high resolution transmission electron microscopy on a sample with the formal composition $LaMnO_{3.158}$. Neutron diffraction, in combination with chemical analysis, indicates that the actual composition is $La_{0.95}Mn_{0.95}O_3$. The electron microscopy results indicate that no defect clustering or crystallographic shear occurs. It is concluded that the defect chemistry of $LaMnO_{3+\delta}$ must be described with randomly distributed La and Mn vacancies in equal amounts. © 1994 Academic Press, Inc.

INTRODUCTION

(La, Sr)MnO_3 is of technological importance for use in Solid Oxide Fuel Cells (SOFC) (1), high-temperature electrolyzers, oxygen sensors, and catalysis (2). Most of the important properties are directly related to the defect chemistry, such as catalysis (2), sinter behavior (3, 4), reactivity (5), and electrical conductivity (6).

As a cathode material in SOFC (La,Sr) $MnO_{3+\delta}$ is used in air or pure oxygen, usually at 1273 K. Under these circumstances $La_{1-x}Sr_xMnO_{3+\delta}$ is in the oxygen excess state ($\delta > 0$) for $0 \leq x \leq 0.4$. During cell operation lower oxygen partial pressures can occur due to the depletion of oxygen. To understand the physical properties of (La,Sr)MnO_3 and its behavior in SOFC, and to be able to optimize its behavior, it is important to have a good knowledge of the defect chemistry of (La,Sr)$MnO_{3\pm\delta}$. The solid solution limit of strontium in $La_{1-x}Sr_xMnO_3$ is 70 at.% Sr (7). For application in SOFC compositions up to 50 at.% Sr are considered.

The behavior of the solid solution series $La_{1-x}Sr_x$ MnO_3 is dominated by the end member $LaMnO_{3\pm\delta}$. The defect chemistry of $LaMnO_{3\pm\delta}$ has been the subject of extensive study. The results will be published in five parts. The defect model for $LaMnO_{3-\delta}$ has been treated in part 1 (8). Part 2, this article, considers the structural aspects of the defect chemistry of $LaMnO_{3+\delta}$. In part 3 the density of (La,*A*)$MnO_{3+\delta}$ (*A* = Ca, Sr, Ba) is discussed (9). Defect models to describe the relation between composition (δ) and oxygen partial pressure (p_{O_2}) for $LaMnO_{3+\delta}$ are dealt with in part 4 (10), and, finally in part 5 the temperature dependence and the thermodynamics of defect formation of $LaMnO_{3+\delta}$ and $LaMnO_{3-\delta}$ are discussed (11).

$LaMnO_3$ is the only compound in the La*M*O_3-type (*M* = first row transition metal) compound series that shows noteworthy oxygen excess. Elemans *et al.* (12) studied the structure of $LaMnO_{3.00}$ by neutron diffraction. They found $LaMnO_{3.00}$ to be isostructural with $GdFeO_3$. No La, Mn, or O vacancies or any other defects were observed. Tofield and Scott (13) studied a sample with composition $LaMnO_{3.12}$. They found La and Mn vacancies to be the defects in $LaMnO_{3.12}$, with more La vacancies than Mn vacancies. On the basis of the results of Tofield and Scott (13), Kuo *et al.* (14) have described the defect chemistry of $LaMnO_{3+\delta}$ on the basis of La and Mn vacancies in equal amounts. However, Shimoyama *et al.* (15), also on the basis of the results of Tofield and Scott (13), have described the defect chemistry of $LaMnO_{3+\delta}$ on the basis of only La vacancies in combination with O vacancies. To discriminate between the various models we have studied the structural aspects of the defect chemistry of

* Part 1 has been published in *J. Solid State Chem.* **93**, 212 (1991) as "A New Defect Model to Describe the Oxygen Deficiency in Perovskite-Type Oxides," by authors J. A. M. van Roosmalen and E. H. P. Cordfunke.

0022-4596/94 $6.00

$LaMnO_{3+\delta}$ by neutron diffraction and High-Resolution Transmission Electron Microscopy (HRTEM). The results are presented in this article.

2. EXPERIMENTAL

The $(La,Sr)MnO_{3+\delta}$ powders were prepared by a coprecipitation method described by van Roosmalen and Cordfunke (9). For the neutron diffraction experiment a $LaMnO_{3+\delta}$ sample was annealed at 1570 K for 40 hr in air to obtain good crystallinity. To obtain a high oxygen content another annealing followed at 1055 K for 40 hr. The La : Mn ratio of the sample was determined by Inductively Coupled Plasma (ICP) emission spectroscopy to be 1.00 ± 0.01. The $Mn^{3+} : Mn^{4+}$ ratio was determined by redox titrations to be 2.170 ± 0.001, so the composition of the sample is $LaMnO_{3.158}$. The lattice parameters were determined using standard X-ray powder diffraction techniques: $a = 0.54685(2)$ nm, $\alpha = 60.676(2)°$. Thirty grams of this sample was used in the neutron diffraction experiment.

Neutron diffraction data were collected on the powder diffractometer at the HFR reactor at room temperature, up to 2θ is 155°. Neutrons of wavelength 0.25717(1) nm were obtained after reflection from the (111) planes of a copper crystal. The λ/n contamination had been reduced to less than 0.1% using a pyrolytic graphite filter. Soller slits with a horizontal divergence of 30′ were placed between the reactor and the monochromator and in front of the four ^3He counters.

For the refinement of the structural parameters from the neutron diffractograms the line-profile method described by Rietveld (16) was applied. This program determines the values for the parameters that minimize the function.

$$\chi_\nu^2 = \sum_i w_i \frac{[y_i(\text{obs.}) - y_i(\text{calc.})]^2}{\nu}, \qquad [1]$$

where y_i(obs.) and y_i(calc.) are the observed and calculated values of the ith intensity, and w_i is its statistical weight. ν is the number of observed intensities minus the number of parameters.

For HRTEM the same sample as that for neutron diffraction was used. The powder was ground and mounted on a carbon-coated holey film supported by a Cu grid. HRTEM was performed with a Philips CM30T electron microscope, operating at 300 kV, equipped with a side-entry 60°/30° tilt specimen holder, and a Link energy dispersive X-ray (EDX) detector.

3. NEUTRON DIFFRACTION

With neutron diffraction overall defects can be studied, such as interstitial ions, multiple ions on the same lattice site, and vacancies on normal lattice sites. In this article the attention is focused on the ratio of La to Mn vacancies. All other models did not converge in the refinement, which is in good agreement with the results obtained by Tofield and Scott (13). There are a number of models that can be differentiated:

1. $La_{1-\gamma}Mn_{1-\lambda}O_3$ (La and Mn vacancies, unequal amounts)
2. $La_{1-\gamma}Mn_{1-\gamma}O_3$ (La and Mn vacancies, equal amounts),
3. $LaMn_{1-\gamma}O_3$ (only Mn vacancies),
4. $La_{1-\gamma}MnO_3$ (only La vacancies).

To test these models the following situations were used in the refinements (see also Table I):

1. Refinement of La and Mn occupation numbers, separately.
2. Refinement of La and Mn occupation numbers, constraint to be equal.
2a. La and Mn occupation numbers, fixed at 0.95.
3. La fixed at 1.00, refinement of Mn.
3a. La fixed at 1.00, Mn occupation fixed at 0.90.
3b. Refinement of La, Mn occupation fixed at 0.90.
4. Mn fixed at 1.00, refinement of La.
4a. Mn fixed at 1.00, La occupation fixed at 0.90.
4b. Refinement of Mn, La occupation fixed at 0.90.

In addition to the La and Mn site occupancy, temperature factors, scale factors, oxygen position, halfwidth parameters, zeropoint, and cell parameters were also refined. In models 2a, 3a, and 4a the composition is adjusted to the results of the chemical analysis, an oxygen content of 0.158. For model 2a the adjustment has to be made according to $La_{3/(3+\delta)}Mn_{3/(3+\delta)}O_3$, for model 3a according to $LaMn_{(3-2\delta)/3}$, and for model 4a to $La_{(3-2\delta)/3}MnO_3$.

Refinement of models 1, 2, 2a, and 4 results in the same R-factors and residuals within the accuracy of neutron diffraction. R-factors and residuals of models 3, 3a, and 4a are somewhat larger. Models 3b and 4b do not give an improvement to models 3 and 4, respectively. The

TABLE I
Refinement of the Neutron Diffraction Results, According to Various Overall Defect Models for $LaMnO_{3+\delta}$

Model	La occupation	Mn occupation	R/%	Residual
1	0.962(7)	0.971(12)	0.63	6.91
2	0.965(5)	0.965(5)	0.67	6.90
2a	0.950	0.950	0.85	7.04
3	1.000	0.939(11)	1.08	7.36
3a	1.000	0.895	1.28	7.58
3b	0.983(7)	0.895	1.25	7.49
4	0.955(6)	1.000	0.68	6.99
4a	0.895	1.000	1.69	8.71
4b	0.895	1.011(12)	1.70	8.71

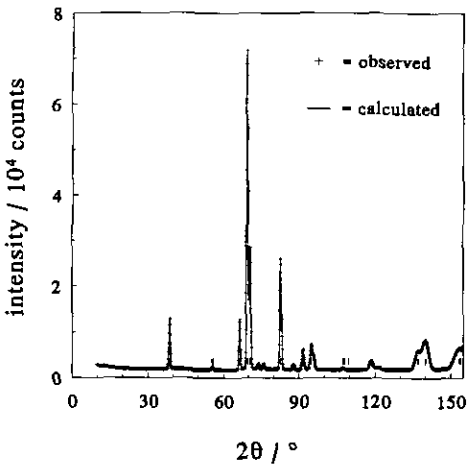

FIG. 1. Powder neutron diffraction results on a sample with the formal composition $LaMnO_{3.158}$. The calculated diagram is based on the model with La and Mn vacancies in equal amounts, $La_{0.95}Mn_{0.95}O_3$.

contribution of La to the refinement is larger than that of Mn. This explains the larger errors in the Mn occupation and that the La occupation in models 4 and 2a is almost the same. The combination of neutron diffraction and chemical analysis leads to model 2a as the best way to describe the defects in $LaMnO_{3+\delta}$.

It should be noted that if there would be an unequal distribution of the metal ion vacancies over the La and Mn sites, phase separation of either La_2O_3 or Mn_2O_3 would be found. Neither these phases, nor any other La or Mn containing phases besides $LaMnO_{3+\delta}$, were observed by neutron diffraction, or by HRTEM (see paragraph 4).

The refinement was performed in the same rhombohedral space group as that used by Tofield and Scott (13), $R\bar{3}c$. A plot of the diffraction pattern, observed and calculated according to model 2a, is shown in Fig. 1. The refined lattice parameters, atomic coordinates, temperature factors, and occupation numbers are listed in Table II. The lattice parameters are in good agreement with the results obtained by X-ray diffraction (paragraph 2).

TABLE II

Lattice Parameters, Atomic Coordinates, Temperature Factors (B), and Occupation Numbers for Model 2A, $La_{0.95}Mn_{0.95}O_3$ in the Rhombohedral Space Group $R\bar{3}c$, $Z = 2$.

Atom		x	y	z	B	Occupation number
2 La	2(*a*)	0.25	0.25	0.25	1.05(5)	1.90
2 Mn	2(*b*)	0.0	0.0	0.0	0.16(12)	1.90
6 O	6(*e*)	−0.3019(2)	0.8019(2)	0.25	1.10(5)	6.00

$a = 0.54698(1)$ nm, $\alpha = 60.659(1)°$

4. ELECTRON MICROSCOPY

HRTEM was performed on the same sample that was used for neutron diffraction, $LaMnO_{3.158}$. If the defects would interact and form small clusters this would lead to diffuse scattering in electron diffraction images. If the defects would cluster, forming extended defects, this would be visible by high resolution electron microscopy as well as by electron diffraction (diffuse scattering). If the uptake of extra oxygen would lead to the formation of microdomains, new phases, structural intergrowth, or crystallographic shear, as in $La_5Ti_5O_{17}$ (17), it should be possible to visualize this with HRTEM.

However, in whatever direction the crystallites were orientated, no defects in the lattice could be detected. A typical diffraction pattern and a typical HRTEM recording of $LaMnO_{3.158}$ are shown in Figs. 2 and 3, respectively. No diffuse streaking is visible in the diffraction patterns (Fig. 2) indicating the absence of defect interaction. Also, only perfect HREM images are observed without any crystallographic shear or other extended structural changes. All this indicates that the defects in $LaMnO_{3+\delta}$ are randomly distributed.

EDX element analysis was done on about 100 crystal fragments, chosen randomly. Six percent of the crystals show a significant deviation from the average La : Mn composition (4% Mn richer and 2% La richer). From these results no definite conclusion can be drawn on the La : Mn ratio except that it must be close to unity.

It is noteworthy that no other phases besides $LaMnO_{3+\delta}$ ($=La_{1-\gamma}Mn_{1-\gamma}O_3$) were detected by HRTEM. The uptake of oxygen by $LaMnO_{3+\delta}$ is a relatively fast, reversible process. If the defect chemistry of $LaMnO_{3+\delta}$ can be described with a (partial) elimination of La or Mn ($La_{(3-2\delta)/3}MnO_3 + (\delta)/3La_2O_3$ or $LaMn_{(3-2\delta)/3}O_3 + (\delta/3)Mn_2O_3$, respectively) very small La or Mn rich regions would be formed within the crystallites leading to strain. No strain was observed by HRTEM.

5. DISCUSSION

Neutron diffraction and HRTEM on a sample with the formal composition $LaMnO_{3.158}$ have shown that the uptake of extra oxygen in $LaMnO_{3+\delta}$ is accommodated by La and Mn vacancies that occur probably in equal amounts. Density measurements (9) indicate that the density of $LaMnO_{3+\delta}$ is constant as a function of δ. This is in accordance with the assumption that La and Mn vacancies occur in equal amounts. The La_2O_3–Mn_2O_3 phase diagram (18) shows that the perovskite-type phase $LaMnO_{3+\delta}$ can occur with a La : Mn ratio smaller than unity as well as a La : Mn ratio larger than unity. This supports the conclusion that in $LaMnO_{3+\delta}$, with a La : Mn ratio of unity, both La and Mn vacancies occur in equal

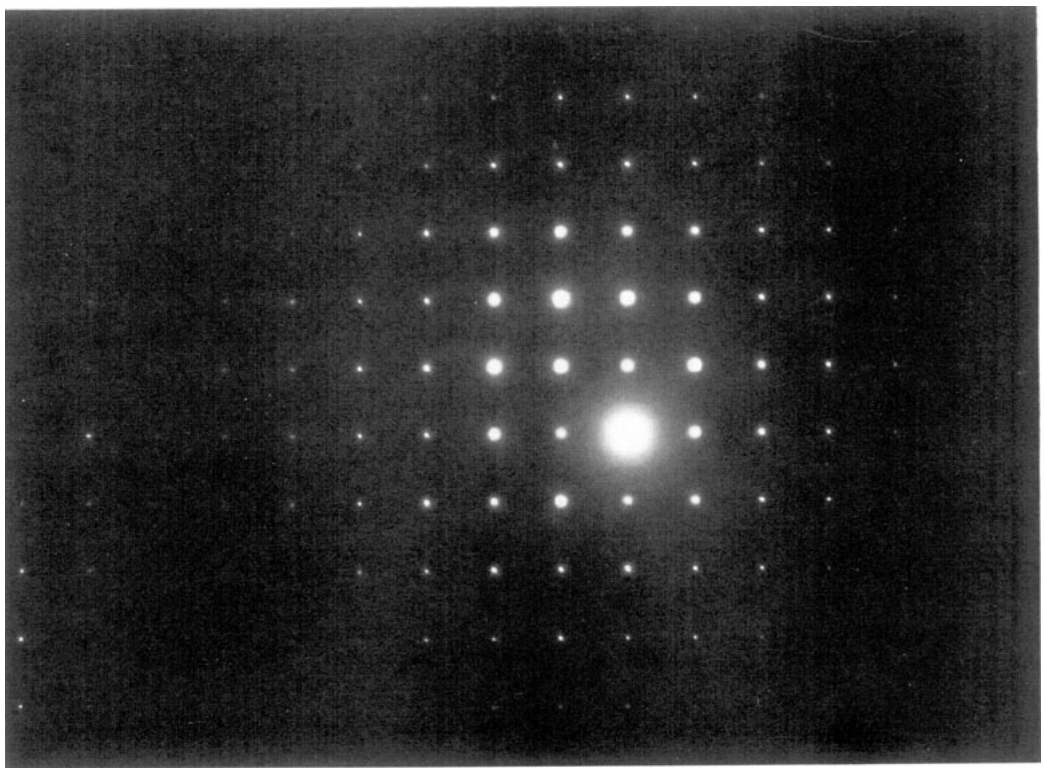

FIG. 2. Typical electron diffraction recording of $LaMnO_{3.158}$ along [100] of the quasi cubic perovskite-like unit cell, showing a nearly perfect rhombohedral reciprocal lattice without any streaking, indicating the absence of defect clustering.

amounts. The overall defect reaction on the basis of La and Mn vacancies in equal amounts can be written:

$$LaMnO_3 + \frac{\delta}{2}O_2 =$$

$$(La\square_{\delta/3})(Mn\square_{\delta/3})O_{3+\delta} = \quad (2)$$

$$\frac{3+\delta}{3}\{(La_{3/(3+\delta)}\square_{\delta/(3+\delta)})(Mn_{3/(3+\delta)}\square_{\delta/(3+\delta)})O_3\}.$$

This implies that the formal notation for $LaMnO_{3+\delta}$ should be $La_{1-\gamma}Mn_{1-\gamma}O_3$ (with $\gamma = \delta/(3+\delta)$), but for clarity this is not used. The overall model can be used conveniently to describe the actual defect chemistry of $LaMnO_{3+\delta}$, as discussed in part 4 (10).

There is a very important difference between our results and the results obtained by Tofield and Scott (13). In a sample with the formal composition $LaMnO_{3.12}$, Tofield and Scott (13) have found that there are three times as many La vacancies as Mn vacancies. Van Roosmalen *et al.* (18) studied the lattice parameters of $LaMnO_{3+\delta}$ as a function of δ and with various La : Mn ratios. These lattice parameter evaluations strongly indicate that the La : Mn ratio of the sample used by Tofield and Scott (13) was less than unity, while the lattice parameters of the sample used in this investigation are in good agreement with the lattice parameters obtained on $LaMnO_{3+\delta}$ samples with a La : Mn ratio of unity. This probably explains why Tofield and Scott find an unequal amount of La and Mn vacancies.

Shimoyama *et al.* (15) have used a model with La as well as O vacancies, $La_{0.9}MnO_{2.85+\delta}$, to describe the defect chemistry of $LaMnO_{3+\delta}$. If this were the right model, for large values of δ (like in the sample used in this work) hardly any oxygen vacancies would be present. At large values of δ the model of Shimoyama *et al.* (15) resembles model 4a. The larger *R*-factor and residual in comparison to the model 2a density measurements (9) and the neutron diffraction results of Elemans *et al.* (12) indicate that the model of Shimoyama *et al.* (15) is probably incorrect.

It was pointed out by Mrowec (19) that, in general, at defect concentrations exceeding 0.1 at.% there will be interaction between the point defects. Van Roosmalen and Cordfunke (8) have shown that in $LaMnO_{3-\delta}$ interaction between point defects leads to the formation of defect clusters. The defect concentrations in $LaMnO_{3+\delta}$ are larger than in $LaMnO_{3-\delta}$, nevertheless there are no indications that defect clusters are formed.

$FeO_{1+\delta}$ is a compound in which the oxygen excess is also compensated by metal-ion vacancies (20, 21). The defect concentrations are comparable with $LaMnO_{3+\delta}$,

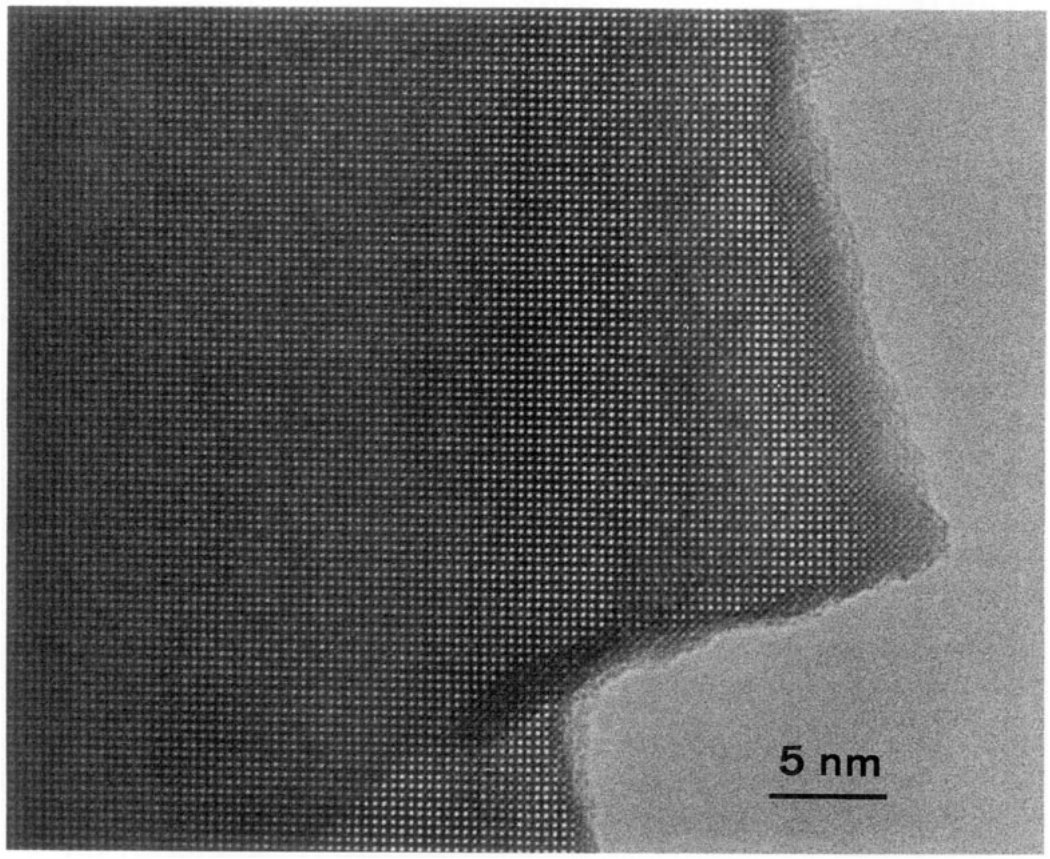

FIG. 3. Typical HRTEM recording of $LaMnO_{3.158}$, showing a perfect lattice along [100] of the quasi cubic unit cell.

but in contradiction to $LaMnO_{3+\delta}$ in $FeO_{1+\delta}$ defect clusters are formed, because Fe^{3+} can occupy tetrahedral sites. A closer look at the perovskite structure of $LaMnO_3$ (Fig. 4) reveals that from an electrostatic point of view it is very unlikely that, like in $FeO_{1+\delta}$, defect interactions lead to defect clusters in $LaMnO_{3+\delta}$. The $LaMnO_3$ perovskite-type structure is a closed-packed LaO_3 lattice with Mn ions in the octahedral sites that are completely surrounded by oxygen ions. The possible sites for interstitial ions (tetrahedral and octahedral) are surrounded by negatively charged ions (oxygen) as well as by positively charged ions (lanthanum). It is thus very hard to incorporate charged particles into these sites. Due to the differences in ionic radii between lanthanum and manganese, it is unlikely that lanthanum occupies manganese sites or vice versa in significant amounts.

As can be seen from Fig. 1 there are three reflections (around 74.0, 76.1, and 88.0° 2θ), with small intensities, that cannot be described in the present unit cell. These reflections do not come from any known form of lanthanum or manganese oxide. From the La_2O_3–Mn_2O_3 phase diagram (18) it is known that there are no other phases that contain La as well as Mn in air besides the perovskite-

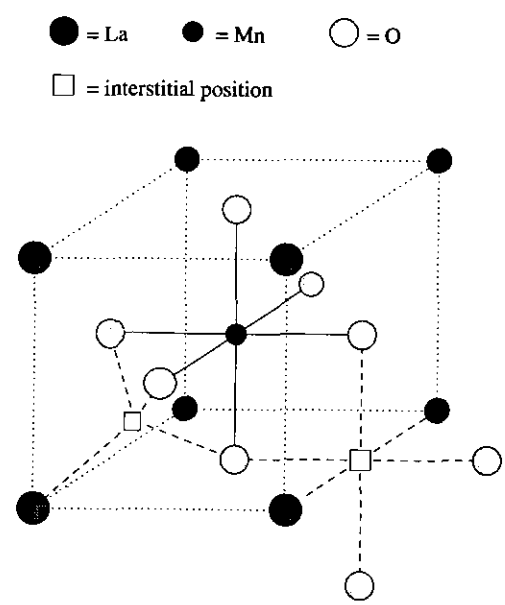

FIG. 4. Schematic drawing of the perovskite structure of $LaMnO_3$. Possible sites for interstitial atoms that may lead to cluster formation are indicated.

type $LaMnO_3$ phase. The three reflections probably result from doubling of the unit cell, although one of the reflections is 0.3° 2θ apart from the position calculated by doubling the lattice parameters. Elemans *et al.* (12) and Tofield and Scott (13) have also found some weak reflections that they ascribe to doubling of the unit cell. Guinier–de Wolff recordings and electron diffraction also indicate doubling of the unit cell (18). We have tried to refine the doubled unit cell, but the three reflections contribute too little for the refinement program to converge. Doubling of the cell is probably the result of a change in one or two of the coordinates of one or two of the eight possibly different oxygen ions in the doubled cell.

ACKNOWLEDGMENT

The authors thank W. L. IJdo for preparing the neutron diffraction sample, P. van Vlaanderen for determining the lattice parameters, and Dr. D. J. W. IJdo of Leiden University for helpful discussions.

REFERENCES

1. J. P. P. Huijsmans, E. J. Siewers, F. H. van Heuveln, and J. P. de Jong, *in* "Proc., Second International Symposium on Solid Oxide Fuel Cells, Athens, 1991" (F. Grosz, P. Zegers, S. C. Singhal, and O. Yamamoto, Eds.), pp. 113–118.
2. R. J. H. Voorhoeve, J. P. Remeika, L. E. Trimble, A. S. Cooper, F. J. Disalvo, and P. K. Gallagher, *J. Solid State Chem.* **14,** 395 (1975).
3. J. A. M. van Roosmalen, J. P. P. Huijsmans, and E. H. P. Cordfunke, *in* "Proc., Second International Symposium on Solid Oxide Fuel Cells, Athens, 1991" (F. Grosz, P. Zegers, S. C. Singhal, and O. Yamamoto, Eds.), pp. 507–516.
4. J. A. M. van Roosmalen, E. H. P. Cordfunke, and J. P. P. Huijsmans, *Solid State Jonics* **66,** 285 (1993).
5. J. A. M. van Roosmalen and E. H. P. Cordfunke, *Solid State Ionics* **52,** 303 (1992).
6. J. A. M. van Roosmalen, J. P. P. Huijsmans, and L. Plomp, *Solid State Ionics* **66,** 279 (1993).
7. G. H. Jonker, *Physica* **22,** 707 (1956).
8. J. A. M. van Roosmalen and E. H. P. Cordfunke, *J. Solid State Chem.* **93,** 212 (1991).
9. J. A. M. van Roosmalen and E. H. P. Cordfunke, *J. Solid State Chem.* **110,** 106 (1994).
10. J. A. M. van Roosmalen and E. H. P. Cordfunke, *J. Solid State Chem.* **110,** 109 (1994).
11. J. A. M. van Roosmalen and E. H. P. Cordfunke, *J. Solid State Chem.* **110,** 113 (1994).
12. J. B. A. A. Elemans, B. van Laar, K. R. van der Veen, and B. O. Loopstra, *J. Solid State Chem.* **3,** 238 (1971).
13. B. C. Tofield and W. R. Scott, *J. Solid State Chem.* **10,** 183 (1974).
14. J. H. Kuo, H. U. Anderson, and D. M. Sparlin, *J. Solid State Chem.* **83,** 52 (1989).
15. J. Shimoyama, J. Mizusaki, and K. Fueki, *"Fall Meeting, Chem. Soc. Japan,* 3Q06 (1986)," quoted by J. Mizusaki and H. Tagawa, *in* "International Symposium on Solid Oxide Fuel Cell, Nagoya, 1989," pp. 65–70.
16. H. M. Rietveld, *J. Appl. Crystallogr.* **2,** 65 (1969).
17. T. Williams, H. Schmalle, A. Reller, F. Lichtenberg, D. Widmer, and G. Bednorz, *J. Solid State Chem.* **93,** 534 (1991).
18. J. A. M. van Roosmalen, P. van Vlaanderen, E. H. P. Cordfunke, W. L. IJdo, and D. J. W. IJdo, *J. Solid State Chem.,* submitted for publication.
19. S. Mrowec, *Ceramurgia Int.* **4,** 47 (1978).
20. J. Nowotny and M. Rekas, *J. Am. Ceram. Soc.* **72,** 1221 (1989).
21. M. J. Radler, J. B. Cohen, and J. Faber, Jr., *J. Phys. Chem. Solids* **51,** 217 (1990).